Stopping Set Analysis for Polar-Polar Concatenated Codes Under BP Decoding

Ziyuan Zhu, *Student Member, IEEE,* and Paul H. Siegel, *Life Fellow, IEEE*

***Abstract*—This paper investigates properties of polar-polar concatenated codes and their potential applications. We start by reviewing previous work on stopping set analysis for conventional polar codes, which we extend in this paper to concatenated architectures. Specifically, we present a stopping set analysis for the factor graph of concatenated polar codes, deriving an upper bound on the size of the minimum stopping set. To achieve this bound, we propose new bounds on the size of the minimum stopping set for conventional polar code factor graphs. The tightness of these proposed bounds is investigated empirically and analytically. We show that, in some special cases, the exact size of the minimum stopping set can be determined with a time complexity of $O(N)$, where N is the codeword length. The stopping set analysis motivates a novel construction method for concatenated polar codes. This method is used to design outer polar codes for two previously proposed concatenated polar code architectures: augmented polar codes and local-global polar codes. Simulation results with BP decoding demonstrate the advantage of the proposed codes over previously proposed constructions based on density evolution (DE).**

***Index Terms*—Polar codes, concatenated polar codes, local-global decoding, stopping sets, belief propagation.**

I. Introduction

POLAR codes, introduced by E. Arıkan [1], occupy a unique place in the history of error correction codes as the first family of codes to achieve the Shannon capacity of arbitrary binary symmetric memoryless channels (BSMs). The code construction starts from a *channel transformation*, where N synthesized bit-channels $W_N^{(i)}$, i=0, 1, ..., $N-1$ are obtained by applying a linear transformation to N independent copies of a BSM channel W. As the block length N goes to infinity, the synthesized bit-channels become either noiseless or completely noisy. A polar code carries information on the least noisy bit-channel positions and freezes the remaining ones to a predetermined value, usually chosen to be zero. Arıkan [2] also introduced the concept of systematic polar encoding, achieved through the solution of linear encoding equations that ensure the codewords contain the information bits at designated positions.

Manucript received MM DD, YYYY; revised MM DD, YYYY. The associate editor coordinating the review of this paper and approving it for publication was NAME.

The authors are with the Electrical and Computer Engineering Department, University of California San Diego, La Jolla, CA 92093, USA (e-mail: {ziz050, psiegel}@ucsd.edu).

The material in this paper was presented in part at the IEEE International Symposium on Information Theory (ISIT), 2024.

This work was supported in part by the National Science Foundation under grants CCF-1764104, CCF-2212437, and CCF-2416362.

Digital Object Identifier xx.xxxx/xxxxxxx.xxxx.xxxx

Code concatenations have been proposed to improve the error correction performance of polar codes. In particular, polar codes have been concatenated with various auxiliary codes, including parity-check codes [3], CRC codes [4], low-density parity-check (LDPC) codes [5], and Reed-Solomon codes [6]. Expanding upon the enhanced belief propagation construction of Guo et al. [7], Elkelesh et al. [8] introduced an augmented polar code architecture that concatenates two polar codes, using an outer auxiliary polar code to further protect the semipolarized bit-channels within the inner polar code. Compared to other augmented polar codes, such as polar-LDPC codes, polar-polar augmented codes provide greater flexibility in both code design and hardware implementation. For instance, adjusting the code rate is simpler with polar codes than with LDPC codes. In polar-polar codes, one can simply modify the frozen positions of the outer codes, inner codes, or both. In contrast, changing the rate of polar-LDPC codes requires redesigning the outer LDPC codes, resulting in different hardware implementations. In the same work [8], they also suggested connecting several inner polar codes through a single auxiliary polar code, offering the flexibility of codeword lengths other than a power of two. Motivated by practical applications in data storage and low-latency communication systems, Zhu et al. [9] proposed an architecture for polar codes offering local-global decoding. In this scheme, a codeword comprising several inner polar codes is concatenated with a systematic outer polar code, thus enabling both local decoding of the inner codes and global decoding of the codeword.

The belief propagation (BP) decoder for polar codes was introduced to increase throughput through a pipelined decoding process [10]. While the BP decoder surpasses the error rate performance of the original successive-cancellation (SC) decoder, it falls short of the SC-list (SCL) decoder [4]. To improve the performance of BP decoding, a method is proposed in [11] to sparsify the dense parity check matrix. Simulation results show that the BP decoding based on the sparsified Tanner graph is particularly effective for short code lengths. The BP-list (BPL) decoder [12], which incorporates different permutation patterns of BP decoding units, significantly enhances error rate performance, bridging the performance gap between BP-based and SC-based decoders. However, how to select the optimal permutation list is still an open problem. It was shown in [13] that better performance can be obtained by selecting L permutations from those with the smallest error probability bound.

Polar codes and Reed-Muller (RM) codes share the same basic encoding matrix before selecting the information set: RM codes select rows according to their Hamming weights,

while polar codes select rows by comparing their associated Bhattacharyya parameters [1]. Another frozen set selection method, introduced by Mori et al. [14], uses density evolution (DE) to analyze BP results for each decoding tree corresponding to the SC decoding process. The high computational complexity of DE motivated the Gaussian approximation (GA) algorithm [15], which assumes that the log-likelihood ratio (LLR) distribution corresponding to each variable node is a Gaussian with mean m and variance $\sigma^2 = 2m$, thus reducing the convolution of densities to a one-dimensional computation of mean values. In [16], Dai et al. proposed a modification to GA to address the performance loss incurred when applying GA to long polar codes.

An important characteristic of polar codes is that the bit-channel orderings are channel-dependent. Although no general rule is known for completely ordering the bit-channels of a general BSM channel, some partial orders (POs) that are independent of the underlying channel have been found for selected bit-channels [14], [17], [18]. In [14], an ordering applicable to bit-channels with different Hamming weights was presented. The Hamming weight of $W_N^{(i)}$ is defined as the number of ones in the binary expansion of i. The ordering states that a bit-channel $W_N^{(j)}$ is stochastically degraded with respect to $W_N^{(i)}$ if the positions of 1 in the binary expansion of j are a subset of the positions of 1 in the binary expansion of i. The ordering in [17] and [18] compared bit-channels with the same Hamming weight. It was based on the observation that a bit-channel $W_N^{(j)}$ is stochastically degraded with respect to $W_N^{(i)}$ if j is obtained by swapping a more significant 1 with a less significant 0 in the binary expansion of i. Both of these orderings are partial, in the sense that not all bit-channel pairs $(W_N^{(i)}, W_N^{(j)})$ are comparable. A more general investigation of POs for polar codes can be found in [19].

In [20], the hybrid RM-polar code construction and stable permutation set were jointly optimized for BP list decoding. The code construction selectively exchanges bit-channels with lower Hamming weight indices and relatively high polarization weight with bit-channels having higher Hamming weight indices and relatively low polarization weight. Taking advantage of bit-channel POs, the construction complexity is shown to be sublinear. The stable permutations, inspired by the selection criterion in [13], preserve a specified information set and preserve the error probability upper bound.

While design methods based on the Bhattacharyya parameters, DE, and GA were originally used in the context of SC decoding, they have also been applied to code design for BP decoding. Eslami et al. [5] introduced a construction method based on stopping sets in the sparse polar code factor graph, aimed at increasing the stopping distance of the polar code. They provided empirical evidence showing improved performance under BP decoding, compared with the conventional code design.

Iterative decoding is naturally suited for concatenated polar codes, as it leverages the decoding capability of the outer codes to correct errors in the inner codes. In this paper, we investigate BP decoders for concatenated polar code architectures. Since stopping sets are well-established for evaluating the performance of BP decoders, we focus on analyzing stopping sets within these architectures. The analysis of stopping sets in the concatenated factor graph suggests a novel code construction method that identifies promising information sets for the outer code. Error rate simulations demonstrate that the proposed method can improve the performance of augmented and local-global polar codes. Portions of this paper were presented in [21], [22].

The paper is organized as follows. Section II briefly reviews background results and notation used in the rest of the paper. In Section III, we provide the stopping set analysis for concatenated polar codes, and we emphasize the importance of finding the minimum stopping set within the conventional polar code factor graph that includes certain information nodes. Section IV presents lower and upper bounds on the size of these minimum stopping sets, while Section V provides exact calculations for specific information node choices on the leftmost stage of the polar code factor graph. In Section VI, we propose an outer code design method based on stopping set analysis for concatenated polar code architectures. Finally, Section VII concludes the paper.

II. Preliminaries

A. Polar Codes and Systematic Polar Codes

In conventional polar code design, N independent copies of a channel W are combined in a recursive manner into a vector channel W_N, which is then split into N channels $W_N^{(i)}$, $0 \le i \le N-1$, referred to as bit-channels. The Bhattacharyya parameter $Z(W_N^{(i)})$ is used to identify the quality of bit-channel i. A polar code of rate $R{=}\frac{K}{N}$ selects the K most reliable bit-channels (with the smallest $Z(W_N^{(i)})$) to input information bits, and the remaining bit-channel inputs are frozen to zero. We use $\mathcal{A}$ to denote the set of information indices, and $\mathcal{F}{=}\mathcal{A}^c$ to denote the frozen indices. Let $G{=}F^{\otimes n}$ be the $N{\times}N$ matrix that is the n-th Kronecker power of $F{=}\begin{bmatrix} 1 & 0 \\ 1 & 1 \end{bmatrix}$, where $n{=}\log_2 N$. The polar encoding process is specified by $x{=}uG$, where $x, u \in \mathbb{F}^N, G \in \mathbb{F}^{N\times N}$.

Arıkan [2] showed that a systematic encoder can be realized that maps information bits to positions in the set $\mathcal{B}{=}\mathcal{A}$ in the codeword x. To be specific, $u_{\mathcal{A}^c}$ is set to 0, $x_{\mathcal{B}}$ is set to the information vector, and $u_{\mathcal{A}}$ and $x_{\mathcal{B}^c}$ are found by solving a system of equations.

B. Concatenated Polar Codes

Our focus in this paper is on concatenated code architectures in which all component codes are polar codes. The augmented and flexible length architectures were introduced in [8].

In an augmented polar code, a short auxiliary outer polar code G_0 is connected to an inner polar code G_1. The encoding structure is illustrated in Fig. 1. The short auxiliary outer polar encoder takes the information bits K_0 and the frozen bits F_0 as inputs, producing a codeword of length N_0. This codeword is then passed through an interleaver π, and the permuted codeword serves as the information bits for the semipolarized channels of the inner polar code. The inner polar encoder

receives three inputs: the information bits K_1 assigned to the good bit channels, the frozen bits F_1 assigned to the frozen bit channels, and the interleaved codeword from the outer polar encoder, which is assigned to the semipolarized bit channels. The inner polar encoder outputs a codeword of length N_1, which is then transmitted over the channel. The rate of the outer code is given by $R_0 = \frac{K_0}{N_0}$, while the overall rate of the augmented structure is $R_{aug} = \frac{K_0+K_1}{N_1}$.

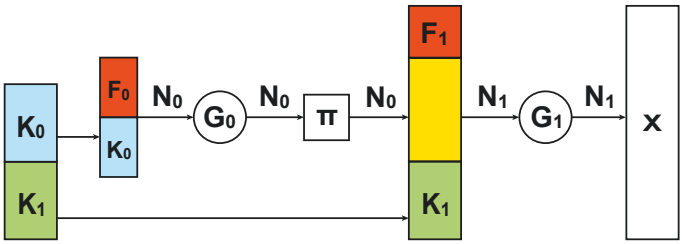

Fig. 1: Encoder of the augmented code.

In the flexible length architecture, two inner codes G_1, G_2 of length N_1, N_2 are coupled through a rate $R_0 = \frac{K_0}{N_0}$ auxiliary outer code G_0. Information words of length K_1, K_2 are assigned to the good bit-channels of the two inner codes, respectively. The outer codeword is divided into two parts which are assigned to the semipolarized bit-channels of the inner codes. The total encoding rate for the flexible length structure is $R_{flex} = \frac{K_0+K_1+K_2}{N_1+N_2}$.

Inspired by the flexible length architecture, the local-global polar code architecture, introduced in [9], connects multiple inner codes $G_1, ..., G_M$ through a systematic outer polar code. We assume these codes have the same length $N_i = N, i = 1, \ldots, M$. A word of K_b information bits is divided into M parts of $K_{b_1}, \ldots, K_{b_M}$ bits that are assigned to the good bit-channels within the inner codes. The K_a outer information bits are divided into M parts of $K_{a_1}, \ldots, K_{a_M}$ bits that are mapped to the semipolarized bit-channels of the M inner codes, respectively. The P_a parity bits of the outer codeword are similarly partitioned into M parts of $P_{a_1}, \ldots, P_{a_M}$ bits and mapped to the remaining semipolarized bit-channels within the inner codes. This architecture supports local decoding of information bits K_{a_i}, K_{b_i} within each inner code G_i, with the option of improved decoding of the M inner codewords via global decoding using the outer code.

C. Stopping Set in Factor Graph

We briefly review the stopping set analysis of polar codes as presented in [5], and we propose some new definitions that will be used throughout the rest of the paper.

1) Notation from Eslami et al. [5]: A stopping set (SS) is a non-empty set of variable nodes such that each neighboring check node is connected to this set at least twice. In this paper, we are particularly interested in the analysis of stopping sets in the factor graph of polar codes. Fig. 2 shows an example of a stopping set in the polar code factor graph, where we also included the corresponding set of check nodes. Denote the factor graph of a polar code of length $N = 2^n$ by T_n. A key observation is the symmetric structure of this graph which

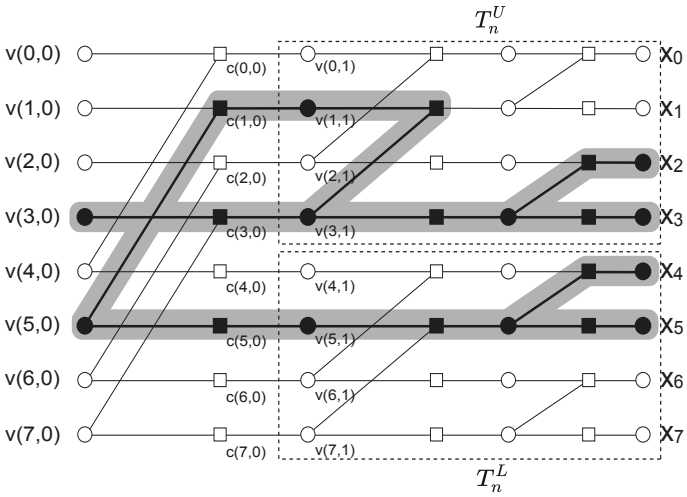

Fig. 2: Normal realization of the factor graph for $N = 8$. An example of a SS is shown with black variable and check nodes.

reflects the recursive construction of the generator matrix: T_n includes two factor graphs equivalent to T_{n-1} as its upper and lower halves, connected together via $v(0,0), v(1,0), ..., v(N-1,0)$ and $c(0,0), c(1,0), ..., c(N-1,0)$. We denote these two subgraphs by T_n^U and T_n^L, as shown in Fig. 2.

A stopping tree (ST) is a SS that contains one and only one information bit, i.e., variable node, on the leftmost stage of the sparse polar code factor graph. For each information bit i, there is a unique stopping tree denoted by $ST(i)$. An example of such a stopping tree is shown in Fig. 3 with black variable nodes. We also included the corresponding set of check nodes in order to visualize the structure of the tree. The size of the leaf set (variable nodes on the rightmost stage) of $ST(i)$ is denoted by $f(i)$. For example, $f(5) = 4$, with the corresponding leaf set $\{x_0, x_1, x_4, x_5\}$.

Only variable nodes on the rightmost stage are observed nodes, with all other variable nodes hidden. The set of observed variable nodes in a SS forms a variable-node SS (VSS). Accordingly, we define a minimum VSS (MVSS) as a VSS with a minimum number of observed variable nodes, among all the VSSs. The size of a MVSS is the stopping distance of the code. For any given index set $\mathcal{J}$, we denote a SS whose information nodes are precisely $\mathcal{J}$ as $SS(\mathcal{J})$. The set of observed variable nodes in a $SS(\mathcal{J})$ is a VSS for $\mathcal{J}$, denoted $VSS(\mathcal{J})$. A minimum size VSS among all the $VSS(\mathcal{J})$ is called a minimum VSS for $\mathcal{J}$, denoted $MVSS(\mathcal{J})$. Note that $SS(\mathcal{J})$, $VSS(\mathcal{J})$ and $MVSS(\mathcal{J})$ may not be unique for a given index set $\mathcal{J}$. The following theorem is taken from [5], and we aim to extend it in Section IV.

Theorem 1. ***(Lower Bound I)*** *Given any set $\mathcal{J}$ of information bits, we have $|MVSS(\mathcal{J})| \geq \min_{j \in \mathcal{J}} f(j)$.*

Proof. The proof can be found in the Appendix of [5]. ■

Define $SD(\mathcal{A}) = \min_{\mathcal{J} \subseteq \mathcal{A}} |MVSS(\mathcal{J})|$ as the stopping distance of a polar code with information set $\mathcal{A}$. Theorem 1 sets a lower bound on the size of a MVSS for a set $\mathcal{J}$ of information

bits. It also implies that the size of a MVSS for a polar code with information set $\mathcal{A}$ is at least equal to $\min_{i\in\mathcal{A}} f(i)$. However, we already know that the leaf set of the stopping tree for any node $i \in \mathcal{A}$ is a VSS of size $f(i)$. The following corollary can be directly established:

Corollary 1. *For a polar code with information bit index $\mathcal{A}$, $SD(\mathcal{A}) = \min_{i\in\mathcal{A}} f(i)$.*

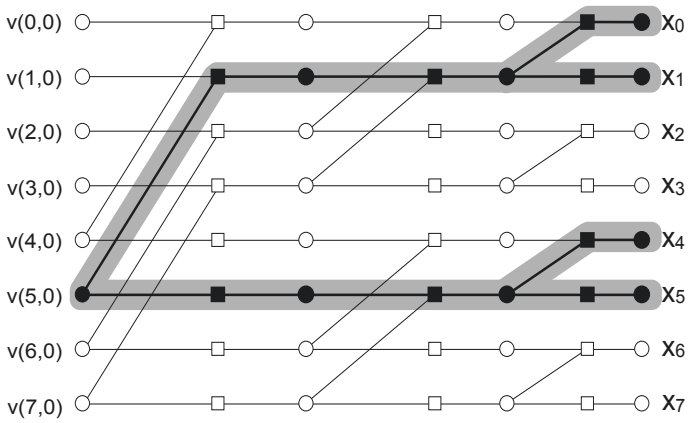

Fig. 3: The stopping tree for v(5,0) is shown with black variable and check nodes.

2) New notation introduced in this paper: Let $i \in \mathbb{Z}_N$ have the binary representation $i_b = i_0, i_1, ..., i_{n-1}$, where $i = \sum_{k=0}^{k=n-1} i_k \times 2^k$, and let $wt(i_b)$ denote the weight of i_b (i.e., the number of 1s). For example, if $i = 6$, then $i_b = 011$ and $wt(i_b) = 2$. According to Fact 5 in [5], for a length-2^n polar code, $f(i) = wt(r_i)$, where r_i is the $(i+1)$-th row of $G = F^{\otimes n}$. Furthermore, it directly follows from the properties of the recursively generated G that $wt(r_i) = 2^{wt(i_b)}$. Thus, for $0 \le i \le 2^n - 1$, the following equation provides a straightforward method to calculate $f(i)$:

$$f(i) = 2^{wt(i_b)}. \tag{1}$$

Given information set $\mathcal{J}$, we use $UT(\mathcal{J}) = \cup_{j\in\mathcal{J}} ST(j)$ to denote the union of all the stopping trees defined by the elements in $\mathcal{J}$, which is also the largest $SS(\mathcal{J})$, with all other $SS(\mathcal{J}) \subseteq UT(\mathcal{J})$, as stated in the following proposition. Fig. 4 gives an example of $UT(\mathcal{J})$ with $\mathcal{J} = \{3, 5\}$. Define the degree of a node as the number of its neighboring nodes. Specifically, the degree of a variable node is the number of its neighboring check nodes, and the degree of a check node is the number of its neighboring variable nodes. In Fig. 4, $c(1,0)$ and $v(1,1)$ have a degree of 2, while $c(1,1)$ and $v(3,1)$ have a degree of 3.

Proposition 1. *Any $SS(\mathcal{J})$ is a subset of $UT(\mathcal{J})$.*

Proof. Assume there exists a node $v(r^*, c^*) \notin UT(\mathcal{J})$ such that $v(r^*, c^*)$ is in some $SS(\mathcal{J})$. If $c(r^*, c^*-1)$ is of degree 2 in the factor graph, then its neighboring variable node in column c^*-1 must be in $SS(\mathcal{J})$. Alternatively, if $c(r^*, c^*-1)$ is of degree 3, then at least one of its two neighboring variable nodes in column c^*-1 is in $SS(\mathcal{J})$. Without loss of generality, assume $v(r^*, c^*-1)$ is in $SS(\mathcal{J})$. Clearly, $v(r^*, c^*-1)$ is a parent of $v(r^*, c^*)$. We can then apply the same process to find the parent(s) in columns c^*-2, c^*-3, and so on, until we reach column 0.

At this point, there must exist a node $v(r^{**}, 0)$ that is a parent of $v(r^*, c^*)$, implying $v(r^*, c^*) \in ST(r^{**})$ and that any $SS(\mathcal{J})$ containing $v(r^*, c^*)$ must also contain $v(r^{**}, 0)$. However, since we assumed $v(r^*, c^*) \notin UT(\mathcal{J})$, it follows that $v(r^{**}, 0) \notin \mathcal{J}$, which contradicts the fact that $v(r^{**}, 0)$ is in $SS(\mathcal{J})$. ∎

A degree-3 check node in $UT(\mathcal{J})$ must lie in the intersection of two stopping trees. We refer to this as an *intersection check node (ICN)*, and we denote the set of these as $ICN(\mathcal{J})$. A leaf that is shared by more than one $ST(i)$, $i \in \mathcal{J}$ is referred to as an *overlapped leaf (OLL)*. The set of overlapped leaves is denoted as $OLL(\mathcal{J})$. The leaves that are associated with exactly one $ST(i)$, $i \in \mathcal{J}$ are called *non-overlapped leaves* and denoted as $nOLL(\mathcal{J})$. For each element in $OLL(\mathcal{J})$, there exists at least one parent ICN. The parent ICN of the leaf indexed by i with the largest column index is called the root ICN of i, denoted as $rICN(i)$. Again taking Fig. 4 as an example, $nOLL(\mathcal{J}) = \{x_2, x_3, x_4, x_5\}$, $OLL(\mathcal{J}) = \{x_0, x_1\}$ and $rICN(0) = rICN(1) = c(1,1)$.

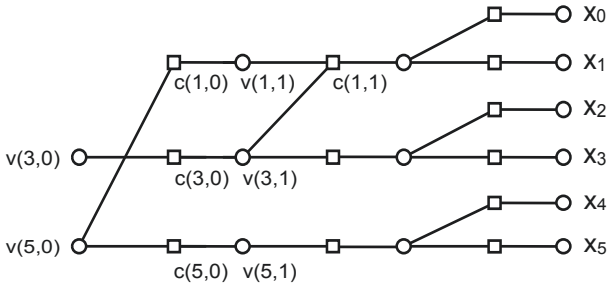

Fig. 4: An example of $UT(\mathcal{J})$ for a set $\mathcal{J}$ of size 2.

III. Stopping set analysis for concatenated polar codes

Consider the augmented polar code structure in Fig. 5, where an inner polar code is concatenated with an outer polar code. Recall that the inner information positions that are connected with the outer code are known as semipolarized channels, and the rest of the inner information bits are assigned to the good bit-channels [8]. To be specific, K_0 information bits are assigned to the auxiliary outer polar code, and an additional K_1 information bits are assigned to the good bit-channels within the inner code. The connection pattern between the outer codeword and the semipolarized bit-channels of the inner code is determined by an interleaver.

Let $v_0(i)$ denote the $(i+1)$-th node on the leftmost stage within the outer factor graph, and let $v_1(j)$ denote the $(j+1)$-th node on the leftmost stage within the inner factor graph. Let $\mathcal{H}_i$ denote the set of inner information nodes such that each element in $\mathcal{H}_i$ is connected to one of the leaves in the stopping tree $ST(i)$ defined on the outer factor graph. Let $MVSS(\mathcal{H}_i)$ be a MVSS (which may not be unique) defined by set $\mathcal{H}_i$ within the inner factor graph. For example in Fig. 5, $\mathcal{H}_2$ is the set of nodes $\{v_1(1), v_1(5)\}$. $MVSS(\mathcal{H}_2)$ is the set

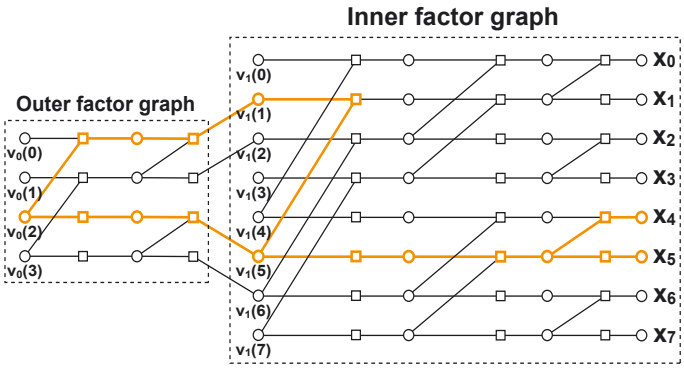

Fig. 5: Augmented structure with N_0=4, N_1=8. Orange nodes represent a SS and $\{x_4, x_5\}$ are a MVSS.

of nodes $\{x_4, x_5\}$. Note that $\{x_0, x_1, x_4, x_5\}$ is also a VSS for $\mathcal{H}_2$, but it is not a minimum VSS.

The information set $\mathcal{J}$ was previously defined as the set of indices of the information nodes. In this section, we slightly modify the definition of $\mathcal{J}$ to represent the information nodes themselves, rather than their indices, to avoid confusion between the elements in the set of outer information nodes and those in the set of inner information nodes. Denote the set of information nodes on the leftmost stage of the outer factor graph that corresponds to K_0 as $\mathcal{J}_{out}$, and denote the set of information nodes on the leftmost stage of the inner factor graph corresponding to K_1 as $\mathcal{J}_{in}$. Define $\mathcal{J}_{total} = \mathcal{J}_{out} \cup \mathcal{J}_{in}$.

Note that there is no valid stopping set within the overall factor graph whose intersection with the union of the leftmost stages of the inner and outer factor graphs is exactly $\mathcal{J}_{total}$. This is because, when $\mathcal{J}_{out}$ is non-empty, some inner information nodes corresponding to semipolarized channels must be included in the stopping set. However, $\mathcal{J}_{in}$ does not include any nodes corresponding to semipolarized channels. For example, in Fig. 5, with $\mathcal{J}_{out} = \{v_0(2)\}$ and $\mathcal{J}_{in} = \emptyset$, $\mathcal{H}_2$ must be part of any stopping set that only contains $\mathcal{J}_{out}$ on the leftmost stage. Therefore, we introduce the following definition: Let $SS'(\mathcal{J}_{total})$ denote a stopping set within the overall factor graph that includes exactly $\mathcal{J}_{out}$ on the leftmost stage of the outer factor graph, and $\mathcal{J}_{in}$ along with some semipolarized nodes, on the leftmost stage of the inner factor graph.

Example 1. *We provide an example of SS' to demonstrate that at least one such set always exists for any given $\mathcal{J}_{total}$. Let $UT(\mathcal{J}_{out})$ represent the union of stopping trees in the outer factor graph, and let $\mathcal{H}_{\mathcal{J}_{out}}$ be the set of inner information nodes, where each element in $\mathcal{H}_{\mathcal{J}_{out}}$ is connected to one of the leaves in $UT(\mathcal{J}_{out})$. Define $\mathcal{J}^* = \mathcal{H}_{\mathcal{J}_{out}} \cup \mathcal{J}_{in}$, and let $UT(\mathcal{J}^*)$ be the union of stopping trees in the inner factor graph. Then, the set $UT(\mathcal{J}_{out}) \cup UT(\mathcal{J}^*)$ forms a valid $SS'(\mathcal{J}_{total})$.*

In the augmented polar code structure, only the variable nodes on the rightmost stage of the inner factor graph are observed nodes. Accordingly, let $VSS'(\mathcal{J}_{total})$ denote a set of observed variable nodes in $SS'(\mathcal{J}_{total})$, and let $MVSS'(\mathcal{J}_{total})$ denote a minimum VSS among all the $VSS'(\mathcal{J}_{total})$. Define $SD'(\mathcal{J}_{total}) = \min_{\mathcal{J} \subseteq \mathcal{J}_{total}} |MVSS'(\mathcal{J})|$ as the stopping distance of the augmented code. This nomenclature is appropriate because $SD'(\mathcal{J}_{total})$ characterizes the minimum number of errors at the receiver that will cause some unrecoverable errors in the BP decoder. We now derive an upper bound on this stopping distance.

We begin by considering a single information node. For an inner information node $i \in \mathcal{J}_{in}$, the leaves of $ST(i)$ are $MVSS'(i)$. Therefore, we continue to use $f(i)$ to characterize the value of $|MVSS'(i)|$ for $i \in \mathcal{J}_{in}$. For an outer information node $i \in \mathcal{J}_{out}$, it can be seen that $\mathcal{H}_i$ must be included in $MVSS'(i)$. Thus, we are interested in determining $|MVSS(\mathcal{H}_i)|$ within the inner factor graph. Clearly, $MVSS(\mathcal{H}_i)$ forms a $VSS'(i)$, thus providing an upper bound on $|MVSS'(i)|$. Let $f_{out}(i) = |MVSS(\mathcal{H}_i)|$. The following theorem then provides an upper bound on $SD'(\mathcal{J}_{total})$.

Theorem 2. *Let $\min(a, b)$ be the function that returns the minimum value of a and b. Then, we have*

$$SD'(\mathcal{J}_{total}) \leq \min(\min_{j \in \mathcal{J}_{out}} f_{out}(j), \min_{j \in \mathcal{J}_{in}} f(j)).$$

Proof. To start with, we point out that $SD'(\mathcal{J}_{total}) \leq \min_{j \in \mathcal{J}_{total}} |MVSS'(j)|$. This inequality arises because it defines a search space that is contained in the search space considered by $SD'(\mathcal{J}_{total})$, which examines all possible combinations of nodes $\mathcal{J} \subseteq \mathcal{J}_{total}$ and selects the smallest $|MVSS'(\mathcal{J})|$. Next, we note that $\min_{j \in \mathcal{J}_{total}} |MVSS'(j)| = \min(\min_{j \in \mathcal{J}_{out}} |MVSS'(j)|, \min_{j \in \mathcal{J}_{in}} f(j))$. Finally, as previously discussed, $f_{out}(j)$ provides an upper bound on $|MVSS'(j)|$ for $j \in \mathcal{J}_{out}$, i.e., $|MVSS'(j)| \leq f_{out}(j)$, thereby completing the proof. ∎

Given that $f(i)$ can be easily calculated by using Proposition 1, it is of interest to determine the value of $f_{out}(i) = |MVSS(\mathcal{H}_i)|$. Since the connection pattern between the inner code and the outer code is determined by an interleaver, knowing $f_{out}(i)$ would be sufficient if we can find $|MVSS(\mathcal{J})|$ for any selection of $\mathcal{J}$ within the inner factor graph. Theorem 1 gives a lower bound on this value. Empirical results, discussed in the next section, show that this bound is loose when $\mathcal{J}$ is randomly chosen (though we will prove that the bound becomes tight for some specific choices of $\mathcal{J}$). However, we will introduce four useful bounds on $|MVSS(\mathcal{J})|$, including one lower bound and three upper bounds.

IV. Bounds on $|MVSS(\mathcal{J})|$

As discussed in the previous section, to compute $f_{out}(i) = |MVSS(\mathcal{H}_i)|$, it suffices to be able to determine $|MVSS(\mathcal{J})|$ for an arbitrary set $\mathcal{J}$ within the conventional polar factor graph. However, finding the exact value is challenging. In this section, we propose four different bounds on $|MVSS(\mathcal{J})|$. The proposed lower bound performs better than the one described in Theorem 1, particularly when $\mathcal{J}$ is randomly chosen, as we will demonstrate through simulation results. Among the three upper bounds, the Encoding Bound has the

lowest time complexity, though it does not perform as well as the others, which will be evident from experiment results. The Deletion Bounds I and II are similar but applicable to different scenarios, which we will discuss later in this section.

A. Lower bound on $|MVSS(\mathcal{J})|$

Let $G_{\mathcal{J}}$ denote the submatrix of the inner encoding matrix $G = F^{\otimes n}$ consisting of the rows that correspond to $\mathcal{J}$. Again taking Fig. 5 as an example, the resulting $G_{\mathcal{H}_2}$ consists of the second and sixth rows of the inner encoding matrix $G = F^{\otimes 3}$. The following theorem, presented in [21], gives a lower bound on the size of $MVSS(\mathcal{J})$.

Theorem 3. ***(Lower Bound II)*** *Given any information set $\mathcal{J}$, we have $|MVSS(\mathcal{J})| \geq g(G_{\mathcal{J}})$, where*

$$g(A_{p\times q}) = \sum_{j=1}^{q} \delta(\sum_{i=1}^{p} a_{ij} - 1) \tag{2}$$

$$\delta(x) = \begin{cases} 1 & \textit{if } x = 0, \\ 0 & \textit{otherwise}. \end{cases} \tag{3}$$

Proof. The proof can be found in the Appendix of [21]. ■

In words, the function $g(\cdot)$ counts the number of columns in a matrix that have weight one. Thus, for any given information indices $\mathcal{J}$ we easily calculate the lower bound on the size of a $MVSS(\mathcal{J})$ by looking at the generator matrix of the polar code.

B. Upper bounds on $|MVSS(\mathcal{J})|$

Given a vector $v = [v_0, v_1, \ldots, v_{n-1}] \in \mathbb{F}^n$, the *support set* of v, denoted as supp(v), is the set of indices where the elements of v are non-zero. Formally, supp(v) $= \{i \in \{0, 1, \ldots, n-1\} \mid v_i \neq 0\}$. For example, for the vector $v = [1, 0, 0, 1, 1]$, the support set is supp(v) = $\{0, 3, 4\}$.

Theorem 4. ***(Encoding Bound)*** *Let u be a length-N binary vector, whose support set is $\mathcal{J}$. Let $x = uG$. Then, the nodes on the rightmost stage that are indexed by the support set of x form a $VSS(\mathcal{J})$, and we have:*

$$|MVSS(\mathcal{J})| \leq wt(x).$$

Proof. In the encoding process of polar codes, all of the variable nodes in the factor graph are set to either 0 or 1. Each check node has an even number of neighboring variable nodes with value 1, in order to satisfy the parity check requirement. If we initialize the variable nodes on the leftmost stage of the factor graph with u, i.e., set nodes in $\mathcal{J}$ to 1 and nodes in $\mathcal{J}^c$ to 0, and update for each variable node on the other stages (which is basically the encoding process), then the value-1 nodes on the rightmost stage will be indexed by the support set of x.

We state that after the encoding process, all the variable nodes with value 1 form a stopping set. The reason is that if a check node is connected with a value-1 variable node, then it must connect to exactly two value-1 variable nodes to satisfy the parity check equations. Thus, we can pick all the value-1 variable nodes on the rightmost stage to form a variable stopping set of $\mathcal{J}$.

Note that the validity of the proof relies on setting the information bits corresponding to $\mathcal{J}$ to 1 and the frozen bits corresponding to $\mathcal{J}^c$ to 0. We use this configuration in order to leverage the encoding process to simplify the formulation of the bound. ■

Fig. 6 gives an example of Theorem 4, where $\mathcal{J} = \{0, 3, 7\}$. The value-1 variable nodes together with their neighboring check nodes are shown in black. In this example, $x = [1, 0, 0, 0, 1, 1, 1, 1]$, and the corresponding $VSS(\mathcal{J}) = \{x_0, x_4, x_5, x_6, x_7\}$.

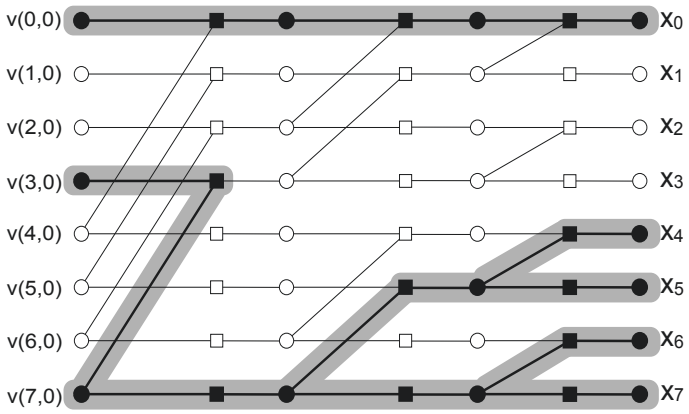

Fig. 6: An example of the Encoding Bound, $\mathcal{J} = \{0, 3, 7\}$.

The following two upper bounds are algorithm-based. From Proposition 1, we know that any $MVSS(\mathcal{J})$ is a subset of $UT(\mathcal{J})$. To find a $MVSS(\mathcal{J})$, we begin by deleting some nodes from the set of leaf nodes in $UT(\mathcal{J})$. When the code length N and $|\mathcal{J}|$ are small, such as when both are less than 32, we can perform an exhaustive search for $MVSS(\mathcal{J})$. For instance, in Fig. 4, the worst-case complexity involves testing all possible deletion patterns in the set of leaf nodes $\{x_0, x_1, x_2, x_3, x_4, x_5\}$, which amounts to $\sum_{k=1}^{k=5} \binom{6}{k} = 62$ combinations.

However, since the time complexity is not polynomial with respect to $|\mathcal{J}|$, a different approach is required for large N and $|\mathcal{J}|$. Instead of randomly selecting combinations, we will need a certain deletion schedule. The following two upper bounds, derived from similar algorithms but employing distinct schedules, are appropriate for different choices of $\mathcal{J}$. Before introducing the upper bounds, we reduce the search space for deletion patterns by observing that $nOLL(\mathcal{J})$ must be included in any $MVSS(\mathcal{J})$, as stated in the following proposition:

Proposition 2. *Given set $\mathcal{J}$ within the factor graph of a polar code, we have $nOLL(\mathcal{J}) \subseteq MVSS(\mathcal{J})$.*

Proof. To see this, suppose that non-overlapped leaf node (nOLL) $x_k \in UT(\mathcal{J})$ belongs only to the stopping tree $ST(i)$, where $i \in \mathcal{J}$. The variable nodes on the branch of $ST(i)$ that traces back to the root node $v(i, 0)$ must also be

non-overlapped. This is because if one of the nodes $v(p,q)$ on that branch is shared by two trees or more, then all the children nodes of $v(p,q)$, i.e., nodes to the right of $v(p,q)$ along the tree $ST(i)$, must be shared nodes, including the leaf node x_k. This contradicts the assumption that x_k is unshared. Since this branch belongs only to $ST(i)$, the result of deleting x_k or any subset of nodes from this branch other than the root node $v(i,0)$ could not produce a stopping set, for this would mean that the remaining subset of nodes in $ST(i)$ would still constitute a stopping tree, call it $ST'(i)$, with root $v(i,0)$. However, this would violate Fact 2 in [5], which states that every information bit has a unique stopping tree. A simple example is shown in Fig. 6, where $\mathcal{J} = \{0,3,7\}$ and $nOLL(\mathcal{J}) = \{x_4, x_5, x_6, x_7\}$. There is no proper $SS(\mathcal{J})$ that does not include $nOLL(\mathcal{J})$. ■

Theorem 5. ***(Deletion Bound I)*** *Let S be the set of variable nodes returned by Algorithm 1. Then S forms a $VSS(\mathcal{J})$, and we have:*

$$|MVSS(\mathcal{J})| \leq |S|$$

Proof. From Proposition 2, we know that $MVSS(\mathcal{J})$ must include $nOLL(\mathcal{J})$. The algorithm attempts to delete some nodes from the set $OLL(\mathcal{J})$ by checking whether the punctured $UT(\mathcal{J})$ can still form a stopping set, i.e., by verifying if any degree-1 check nodes remain (see lines 9-11 in the algorithm). If S is returned by the algorithm, then there exists a punctured subgraph containing $\mathcal{J}$ on the left and S on the right, with some nodes in the middle, which forms a stopping set. ■

Algorithm 1 Find small VSS (Deletion Bound I)

Input: $\mathcal{J}$, N (N is used to initialize the factor graph)
Output: $VSS(\mathcal{J})$

find $OLL(\mathcal{J})$ and $nOLL(\mathcal{J})$
UT $\leftarrow UT(\mathcal{J})$
$VSS(\mathcal{J}) \leftarrow nOLL(\mathcal{J})$
OLL_temp $\leftarrow OLL(\mathcal{J})$
while OLL_temp is not empty **do**
    UT_punc = UT
    pick l with the largest index from OLL_temp
    delete children leaves of $rICN(l)$ from UT_punc
    while Exist a degree-1 CN in UT_punc **do**
        delete this degree-1 CN and its neighbor VN from UT_punc
    end while
    if any VN on the leftmost stage is deleted **then**
        $VSS(\mathcal{J}) = VSS(\mathcal{J}) \cup \{l\}$
        remove l from OLL_temp
    else
        remove all the leaves deleted in this iteration from OLL_temp
        UT = UT_punc
    end if
end while

An example of Algorithm 1 is shown in Fig. 7 with $\mathcal{J} = \{0,3,7\}$ and $N = 8$. $UT(\mathcal{J})$ is shown by the colored nodes (black, green and orange). $nOLL(\mathcal{J}) = \{x_4, x_5, x_6, x_7\}$ and $OLL(\mathcal{J}) = \{x_0, x_1, x_2, x_3\}$. Algorithm 1 first tries to delete x_3 from $OLL(\mathcal{J})$ by trying to delete all the children leaf nodes of $c(3,0)$, which is $rICN(3)$, the rICN of the selected leaf x_3. However, deleting $\{x_0, x_1, x_2, x_3\}$ would result in deletion of $v(0,0)$, so the algorithm labels x_3 as undeletable. The same process applies to x_2 and x_1. The algorithm then moves to x_0. Deleting the only child leaf of $rICN(0)$ yields a structure that forms a stopping set that contains $\mathcal{J}$. As a result, x_0 will be deleted from UT, and the punctured UT is stored for future iterations until all elements in $OLL(\mathcal{J})$ are tried. In this example, since x_0 is the last element, Algorithm 1 will terminate and return the set $\{x_1, x_2, x_3, x_4, x_5, x_6, x_7\}$.

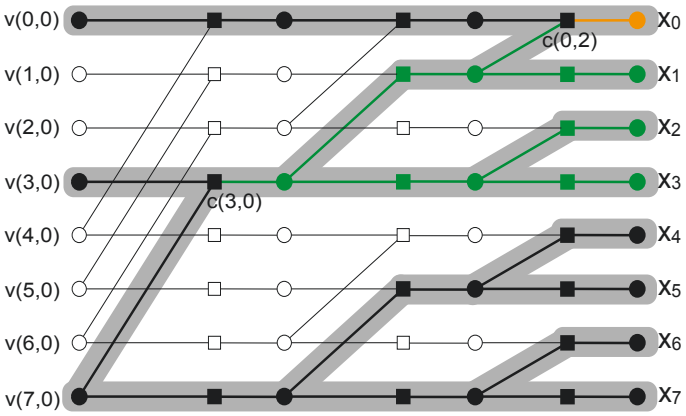

Fig. 7: An example of Deletion Bounds I and II, $\mathcal{J} = \{0,3,7\}$.

In the same example, the exact value of $|MVSS(\mathcal{J})|$ is 5, which is obtained by deleting $\{x_1, x_2, x_3\}$. To improve the performance of Deletion Bound I, we modified Algorithm 1 as follows: Given a leaf node l, instead of identifying $rICN(l)$ and deleting all its children leaves, the new algorithm attempts to delete only the leaf node l itself. Moreover, l is randomly selected instead of being picked according to the largest index. This modified approach is detailed in Algorithm 2. It can be observed that with sufficient attempts using different random deletion seeds, Algorithm 2 can find a $MVSS(\mathcal{J})$, as it effectively performs an exhaustive search. While Algorithm 2 appears to be more adaptive and precise, we will demonstrate through experimental results in Section V that Algorithm 1 performs better for certain choices of $\mathcal{J}$, such as when $\mathcal{J}$ is the information set of a polar codes or a Reed-Muller code.

Theorem 6. ***(Deletion Bound II)*** *Let S be the set of variable nodes returned by Algorithm 2. Then S forms a $VSS(\mathcal{J})$, and we have:*

$$|MVSS(\mathcal{J})| \leq |S|$$

Proof. The same proof as Theorem 5. ■

Consider again the example in Fig. 7. The output of Algorithm 2 has two possible outcomes. If the algorithm selects $l = x_1$ (or x_2, x_3), it will return $\{x_0, x_4, x_5, x_6, x_7\}$

Algorithm 2 Find small VSS (Deletion Bound II)

Input: $\mathcal{J}$, N (N is used to initialize the factor graph)
Output: $VSS(\mathcal{J})$
find $OLL(\mathcal{J})$ and $nOLL(\mathcal{J})$
UT $\leftarrow UT(\mathcal{J})$
$VSS(\mathcal{J}) \leftarrow nOLL(\mathcal{J})$
OLL_temp $\leftarrow OLL(\mathcal{J})$
while OLL_temp is not empty **do**
    UT_punc = UT
    randomly pick l from OLL_temp
    delete l from UT_punc
    while Exist a degree-1 CN in UT_punc **do**
        delete this degree-1 CN and its neighbor VN from UT_punc
    end while
    if any VN on the leftmost stage is deleted **then**
        $VSS(\mathcal{J}) = VSS(\mathcal{J}) \cup \{l\}$
        remove l from OLL_temp
    else
        remove all the leaves deleted in this iteration from OLL_temp
        UT = UT_punc
    end if
end while

with green nodes deleted. If it selects $l = x_0$, it will return $\{x_1, x_2, x_3, x_4, x_5, x_6, x_7\}$ with the orange node deleted. Thus, with a 75% probability, the algorithm provides a bound of 5, and with a 25% probability, it provides a bound of 7.

In practice, we can run the algorithm t times with different random seeds. By repeating the algorithm with varied seeds, we can gather a range of potential outcomes and subsequently select the smallest result as the final upper bound.

C. Simulation results

In this part, we present experiment results that demonstrate the performance of the proposed bounds. The code length for Figs. 8-10 is set to $N = 1024$. The parameter K represents the size of the set $\mathcal{J}$, which corresponds to the number of information bits on the leftmost stage of the factor graph. In Fig. 8, $\mathcal{J}$ is selected to form polar codes designed using Bhattacharyya parameters [1]. In contrast, for Figs. 9 and 10, the set $\mathcal{J}$ is chosen randomly.

In Fig. 8, Deletion Bound I completely aligns with Lower Bound I for all values of K, indicating that these two bounds can accurately determine $|MVSS(\mathcal{J})|$ when $\mathcal{J}$ is chosen to form a polar code. In the following section, we will prove that Lower Bound I can precisely determine the value when $\mathcal{J}$ satisfies certain conditions. Additionally, Fig. 8 shows that Encoding Bound is relatively loose, and while Deletion Bound II does not always yield the exact value of $|MVSS(\mathcal{J})|$, it still provides a fairly good approximation. We ran Algorithm 2 once ($t = 1$) to generate the curve for Deletion Bound II. Lower Bound II is quite loose, as it frequently yields values close to zero.

Fig. 9 compares the proposed bounds when $\mathcal{J}$ is randomly selected. It can be observed that while Deletion Bounds I and II may yield different results, their outputs are very close to one another. Encoding Bound, however, is generally looser than both Deletion Bounds I and II. The performance of the proposed lower bounds differs from Fig. 8: In Fig. 8, where $\mathcal{J}$ is selected to form polar codes, Lower Bound II is loose, whereas in Fig. 9, with randomly chosen $\mathcal{J}$, it is Lower Bound I that is loose and often yields values close to zero.

Fig. 10 compares the performance of Deletion Bound II with different values of t, alongside Deletion Bound I when $\mathcal{J}$ is randomly selected. It can be observed that when the code length N is large, using a small value of t (relative to the size of the search space) has minimal impact on the output of Algorithm 2. Deletion Bounds I and II with a small t produce nearly the same results, suggesting that a one-shot search may suffice for approximating the upper bound of $|MVSS(\mathcal{J})|$.

In Fig. 11, with $N = 32$ and a randomly chosen $\mathcal{J}$, the green dashed line (which coincides with the red line) labeled "$|MVSS|$" represents the exact value of $|MVSS(\mathcal{J})|$, obtained through exhaustive search. It can be observed that Deletion Bound II with $t = 10$ accurately identifies the exact value of $|MVSS(\mathcal{J})|$, while Deletion Bound I is occasionally less tight.

Although the results may differ when Algorithm 2 is run with different random seeds, we emphasize that the outcomes are 'robust' in the sense that they exhibit minimal variation across different random deletion seeds. This is confirmed in Fig. 12, which shows results for $N = 1024$, $K = 256, 512, 768$, with $\mathcal{J}$ selected to form a polar code. In these experiments, Algorithm 2 was run 100 times with different random seeds for each value of K. Instead of picking only the smallest outcome from the 100 trials, we plot all of them in the form of a box plot, with middle half of the results falling within the colored box. The results show little fluctuation.

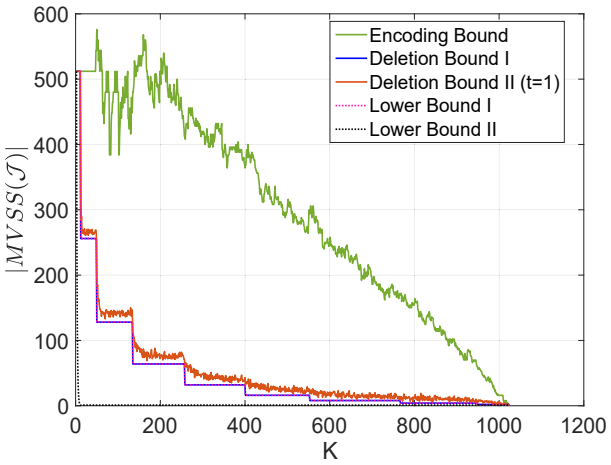

Fig. 8: A comparison of different bounds with $N = 1024$ and $\mathcal{J}$ selected to form polar codes.

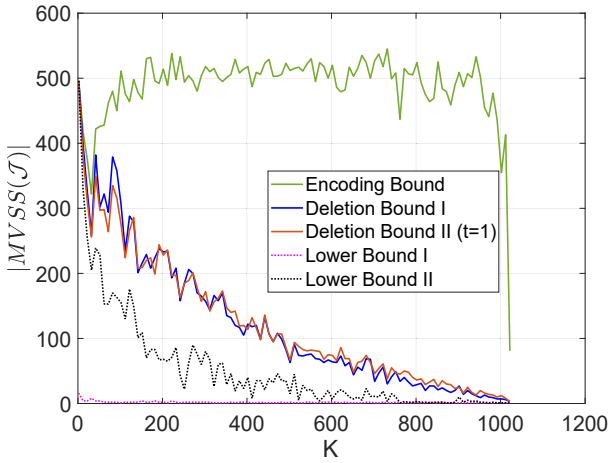

Fig. 9: A comparison of different bounds with $N = 1024$ and randomly selected $\mathcal{J}$.

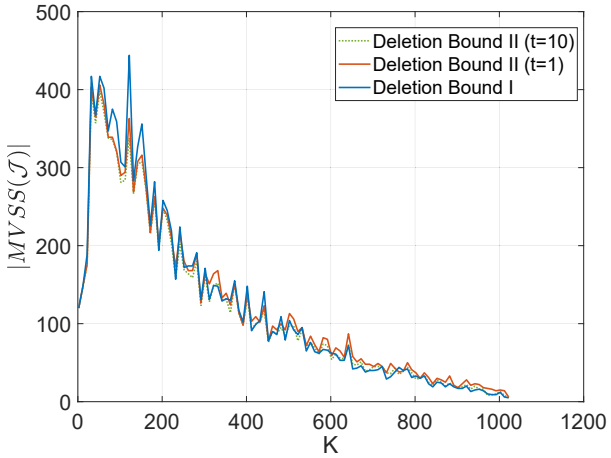

Fig. 10: A comparison of Deletion Bounds I and II with $N = 1024$ and randomly selected $\mathcal{J}$.

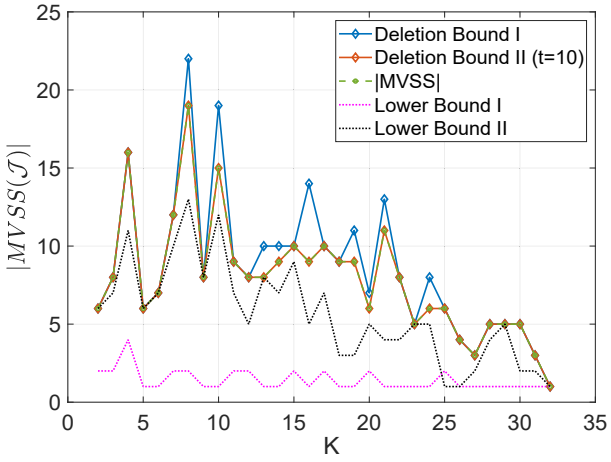

Fig. 11: A comparison of different bounds with $N = 32$ and randomly selected $\mathcal{J}$, alongside the exact value of $|MVSS(\mathcal{J})|$.

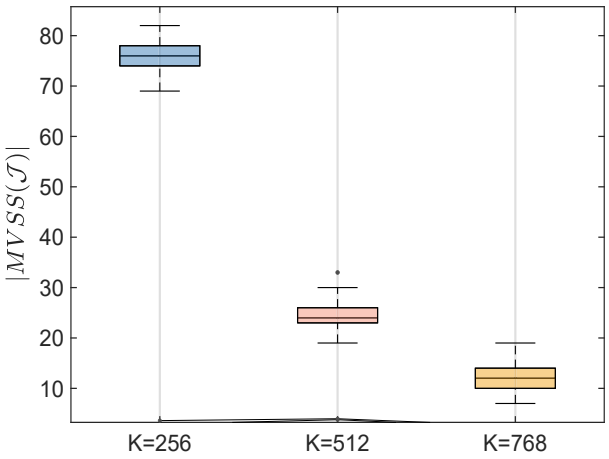

Fig. 12: Box plots of results from Algorithm 2 with different random seeds for $N = 1024$, $K = 256, 512, 768$, and $\mathcal{J}$ selected to form a polar code.

V. $|MVSS(\mathcal{J})|$ FOR SPECIFIC CHOICES OF $\mathcal{J}$

A. Case 1

The following result demonstrates that the bound presented in Theorem 3 is precisely tight in cases where the set cardinality $|\mathcal{J}| = 2$.

Theorem 7. *When* $|\mathcal{J}| = 2$, $|MVSS(\mathcal{J})| = g(G_{\mathcal{J}})$.

Proof. The proof can be found in the Appendix of [21]. ∎

We note that Theorem 7 cannot be extended to the case where $|\mathcal{J}| > 2$. For example in Fig. 13, if $\mathcal{J} = \{1, 6, 7\}$, then the nodes $\{x_0, x_1, x_2, x_4, x_6\}$ are shared leaves. There are two MVSSs for $\mathcal{J}$: $\{x_0, x_3, x_5, x_7\}$ and $\{x_1, x_3, x_5, x_7\}$. Removing the OLLs for $\mathcal{J}$ does not yield an $MVSS(\mathcal{J})$; rather, the size of the resulting VSS provides a lower bound for $|MVSS(\mathcal{J})|$.

B. Case 2

Here we give another condition on $\mathcal{J}$, under which the value of $|MVSS(\mathcal{J})|$ can be determined in $O(N)$, where N is the code length. In words, given information set $\mathcal{J}$ and $f(i)$ for each $i \in \mathcal{J}$ (where $f(i)$ is determined using (1)), $|MVSS(\mathcal{J})|$ can be calculated by selecting the smallest f value. We start with some definitions that are used in the rest of this subsection.

For any given information set $\mathcal{J}$, there always exists an information bit $j \in \mathcal{J}$ whose corresponding stopping tree has the smallest leaf set among all the elements in $\mathcal{J}$. We call such an information bit a *minimum information bit* for $\mathcal{J}$, denoted by $MIB(\mathcal{J})$. Note that there may exist more than one MIB in $\mathcal{J}$. In that case, we pick the one with the largest index. We denote the selected MIB as $MIB^*(\mathcal{J})$. That is, we pick the one which occupies the lowest place in the graph among the MIBs of $\mathcal{J}$.

Let $\mathcal{J}_n$ denote the set of indices on the leftmost stage of the factor graph T_n, and let $\mathcal{J}_n^L$ denote the set of indices on the leftmost stage of T_n^L, such that the variable nodes

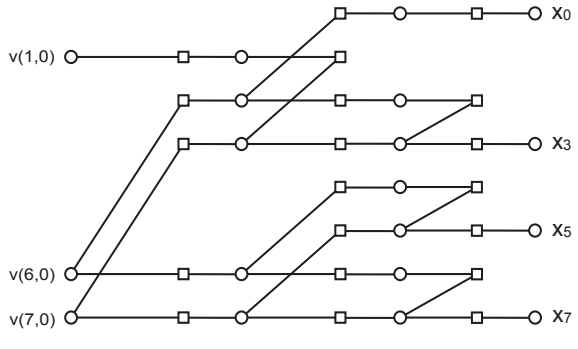

(a) The SS corresponding to $MVSS(\mathcal{J}) = \{x_0, x_3, x_5, x_7\}$.

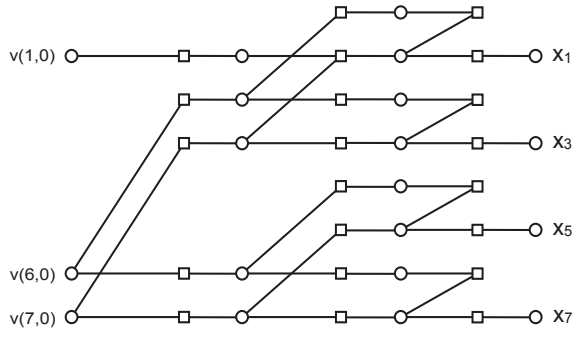

(b) The SS corresponding to $MVSS(\mathcal{J}) = \{x_1, x_3, x_5, x_7\}$.

Fig. 13: Example showing that Theorem 7 does not generalize to $|\mathcal{J}| > 2$.

indexed by $\mathcal{J}_n^L$ on the leftmost stage of T_n^L are in $UT(\mathcal{J}_n)$. Similarly, $\mathcal{J}_n^U$ denotes the set of indices whose corresponding nodes on the leftmost stage of T_n^U are in $UT(\mathcal{J}_n)$. For example in Fig. 4, $\mathcal{J}_n = \{3, 5\}$ (with corresponding nodes $v(3,0), v(5,0)$), $\mathcal{J}_n^L = \{1\}$ (with corresponding node $v(5,1)$) and $\mathcal{J}_n^U = \{1, 3\}$ (with corresponding nodes $v(1,1), v(3,1)$).

Recall that $i, j \in \mathbb{Z}_N$ have binary representations $i_b = i_0, i_1, ..., i_{n-1}$ and $j_b = j_0, j_1, ..., j_{n-1}$, i.e., $i = \sum_{k=0}^{k=n-1} i_k \times 2^k$ and $j = \sum_{k=0}^{k=n-1} j_k \times 2^k$, respectively.

Definition 1. *We write $j \nearrow i$ if there exists $k, k' \in \mathbb{Z}_n$ with $k < k'$ such that*

1) $j_k = 1$ and $j_{k'} = 0$
2) $i_k = 0$ and $i_{k'} = 1$
3) For all $l \in \mathbb{Z}_n \setminus \{k, k'\} : j_l = i_l$

Clearly, if $j \nearrow i$ then $j < i$ and $wt(j_b) = wt(i_b)$.

Definition 2. *Define the following conditions as:*

***(cover condition)** (Definition 7 from [17].) If $j \in \mathcal{J}$ and for all $k \in \mathbb{Z}_n$, we have $j_k = 1 \Rightarrow i_k = 1$ (meaning that i covers j), then $i \in \mathcal{J}$.*

***(swap condition)** (Definition 4 from [17].) If $j \in \mathcal{J}$ and $j \nearrow i$, then $i \in \mathcal{J}$.*

In [17], it is also stated that if i covers j, or $j \nearrow i$, then $W_N^{(j)}$ is stochastically degraded with respect to $W_N^{(i)}$.

Given a set of indices $\mathcal{J}_n$, define $\overline{\mathcal{J}_n} \triangleq \{j \in \mathcal{J}_n | j < 2^{n-1}\}$ and define $\underline{\mathcal{J}_n} \triangleq \{j - 2^{n-1} | j \in \mathcal{J}_n, j \geq 2^{n-1}\}$. In words, $\overline{\mathcal{J}_n}$ is the subset of $\mathcal{J}_n$ that is on the upper-half of the leftmost stage within the factor graph, and $\underline{\mathcal{J}_n}$ is on the lower-half. Similarly, for each $j \in \mathcal{J}_n$ such that $j \geq 2^{n-1}$, we define $\underline{j} = j - 2^{n-1}$. Clearly, we have $f(\underline{j}) = \frac{1}{2} f(j)$ (For detailed proof, see Fact 6 in [5]).

Proposition 3. *If $\mathcal{J}_{n+1}$ satisfies both conditions, then $\underline{\mathcal{J}_{n+1}}$ would also satisfy both conditions.*

Proof. Suppose $j^* \in \underline{\mathcal{J}_{n+1}}$, i^* covers j^*, and $j^* \nearrow i^*$. According to the definition of $\underline{\mathcal{J}_{n+1}}$, we know that $j^* + 2^n \in \mathcal{J}_{n+1}$.

Cover condition: Since $i^* + 2^n$ covers $j^* + 2^n$, and $j^* + 2^n \in \mathcal{J}_{n+1}$, we know that $i^* + 2^n \in \mathcal{J}_{n+1}$. Thus $i^* \in \underline{\mathcal{J}_{n+1}}$.

Swap condition: Since $j^* + 2^n \nearrow i^* + 2^n$, and $j^* + 2^n \in \mathcal{J}_{n+1}$, we know that $i^* + 2^n \in \mathcal{J}_{n+1}$. Thus $i^* \in \underline{\mathcal{J}_{n+1}}$. ■

Theorem 8. *$|MVSS(\mathcal{J})| = \min_{i \in \mathcal{J}} f(i)$ if non-empty set $\mathcal{J}$ satisfies the cover condition and the swap condition.*

Proof. See Appendix. ■

In fact, any decreasing monomial set (see Definition 4 in [18]) satisfies both the cover and swap conditions, as can be directly inferred from the definition and the relationship between the row indices and their corresponding monomials. The information set $\mathcal{A}$ of a polar code is known to be a decreasing monomial set [18], and thus satisfies both conditions. This is also confirmed in [17], where it is shown that the polar information set $\mathcal{A}$ meets these conditions, leading to the following corollary:

Corollary 2. *For a polar code with information set $\mathcal{A}$, $|MVSS(\mathcal{A})| = \min_{i \in \mathcal{A}} f(i)$.*

Consider a binary erasure channel (BEC), where the values of the variable nodes can be 0, 1, or erasure, and a belief propagation (BP) decoder. We examine the erasures on the information nodes after sufficient iterations of BP decoding. Corollary 2 highlights an interesting fact: the probability of erasure for the entire set $\mathcal{A}$ is greater than or equal to the probability of erasure for a single bit $MIB(\mathcal{A})$. The strict inequality may arise when there is more than one MVSS for the set $\mathcal{A}$.

VI. Outer polar stopping set construction

The proposed bounds suggest a practical way to design outer polar codes based on the size of stopping sets. In this section, we focus on Deletion Bound I as an example, given its strong performance among all the proposed bounds on short codes, as shown in Fig. 11. Similar constructions can easily extend to other proposed bounds. Notably, we observe that for the code parameters used in the experiments, the outer codes designed using Deletion Bound I are the same as those designed using Lower Bound II for both the augmented and local-global concatenation architectures. This is surprising given that the two bounds are not identical for these parameters.

A. Construction method

Denote by $d(i)$ the upper bound of $|MVSS(\mathcal{H}_i)|$ obtained by Deletion Bound I. We first initialize an unfrozen set $\mathcal{O}$ for the outer code using the conventional DE, for example. Then we swap a specified number of unfrozen bits $i \in \mathcal{O}$ with the

smallest "stopping distance" $d(i)$ with some positions $j \in \mathcal{O}^c$ such that $d(j) > d(i)$.

Let Q be a length N_0 vector that contains the indices of bit-channels ordered according to channel reliability calculated by DE. The indices are ordered by descending channel reliability, i.e., $Q(1)$ stores the index for the strongest bit channel, $Q(2)$ stores the index for the second strongest, and so on. Let s denote the number of bits we are going to swap. Let K_0 denote the size of the desired unfrozen set. Let $min_s(\cdot)$ be the function that returns the s-th smallest value in a vector, while $min(\cdot)$ returns the smallest value along with its index. Note that s should be chosen such that there are more than s frozen bits that have $d(\cdot)$ value larger than $min_s(d(Q(1)), ..., d(Q(K_0)))$. The detailed swapping algorithm is presented in Algorithm 3. Note that Algorithm 3 can be easily extended to incorporate other bounds by setting $d(i) = |MVSS(\mathcal{H}_i)|$, where $|MVSS(\mathcal{H}_i)|$ represents the value determined by the respective bounds.

Algorithm 3 Outer polar stopping set (OPSS) construction

Input: Q; $d(i)$ for each $i < N_0$; s
Output: designed unfrozen set $\mathcal{O}$

1: $threshold = min_s(d(Q(1)), ..., d(Q(K_0)))$
2: $i \leftarrow 1$
3: **while** $i \leq s$ **do**
4: $\quad [value, index] = min(d(Q(1)), ..., d(Q(K_0)))$
5: $\quad j \leftarrow 1$
6: $\quad$ **while** True **do**
7: $\quad\quad$ **if** $d(Q(K_0 + j)) > threshold$ **then**
8: $\quad\quad\quad Q(index) \leftarrow Q(K_0 + j)$
9: $\quad\quad\quad$ delete $Q(K_0 + j)$ from Q
10: $\quad\quad\quad$ jump to line 14
11: $\quad\quad$ **end if**
12: $\quad\quad j \leftarrow j + 1$
13: $\quad$ **end while**
14: $\quad i \leftarrow i + 1$
15: **end while**
16: Return $\mathcal{O} = Q(1 : K_0)$

We can easily extend Deletion Bound I to the case when M inner codes are connected by a single outer code. For example, assume there are $M = 2$ inner codes and $\mathcal{H}_i = \{\mathcal{H}_i^1, \mathcal{H}_i^2\}$, where $\mathcal{H}_i^1$ and $\mathcal{H}_i^2$ are connected nodes in the first and second inner codes, respectively. Then $d(i) = |MVSS(\mathcal{H}_i^1)| + |MVSS(\mathcal{H}_i^2)|$.

The design method of Algorithm 3 can be extended to the local-global polar code, but some care is needed. The systematic outer code assigns M information vectors K_{a_i}, i=1, ..., M to the M inner codes. Directly applying Algorithm 3 can potentially swap bits K_{a_i} with P_{a_j} ($i \neq j$), causing $[K_{a_i}, K_{a_j}]$ to be assigned to the same inner code. For example, assume the unfrozen set $\mathcal{O} = \{2, 3, 6, 7\}$ represents the most reliable positions according to DE, and $\mathcal{O}^c = \{0, 1, 4, 5\}$. Then, if the partition of $\mathcal{O}$ is according to bit index, the first half of $\mathcal{O}$ will correspond to $K_{a_1} = \{2, 3\}$ and the second half to $K_{a_2} = \{6, 7\}$. If the parity bits are partitioned similarly, we have $P_{a_1} = \{0, 1\}$ and $P_{a_2} = \{4, 5\}$. If, after calculating the $d(i)$ value for each position, we swap positions 2 and 4, this would yield $K_{a_1} = \{3, 4\}$. This assignment is now inconsistent with the local-global architecture because part of K_{a_1} (position 4) is connected with the second inner code. To avoid this problem, one needs to carefully design the partition of the outer codeword in the local-global encoder to ensure that positions in K_{a_i} are only swapped with positions in P_{a_i}. For an example of such a partition, see Example III.2 in [21].

B. Experimental results

Now we give empirical results under BP decoding for augmented and local-global polar codes. The bit-channel ordering is based on DE on the AWGN channel at $E_b/N_0 = 3$ dB. DE is simplified by using Gaussian approximation (GA), using the 4-segment approximation function in [16]. The BP decoding schedules are the same as those in [8] for augmented codes and in [9] for local-global codes. The maximum number of BP decoder iterations is set at 100. In the OPSS design (Algorithm 3), we set the number of bit-channel swaps to $s = 4$. We also include the results for outer codes designed by non-stationary density evolution (NDE), which is another outer code construction method proposed by us in the shorter version of this paper [21]. The NDE algorithm does not assume that the inital LLR distributions to the outer code are identical, as assumed by conventional DE; rather, the LLR distributions coming from the inner code at the rightmost stage of the outer code factor graph correspond to N_0 separate binary symmetric memoryless channels W_i, i=0, ..., N_0−1. In practice, we replace each initial LLR density of the outer code with the empirical LLR density of the corresponding bit-channel of the inner code after ite iterations of BP decoding under assumption of an all-zero codeword. We use $ite = 3$ for the augmented code and $ite = 4$ for the local-global code.

Fig. 14 shows frame error rate (FER) results for augmented code constructions. The outer code length is $N_0 = 64$ with code rate $R_0 = \frac{1}{2}$. The inner code length is $N_1 = 1024$. The design rate of the augmented code is $R_{aug} = \frac{1}{2}$. The connections between the bit-channels of the inner code and the bits of the outer codeword are based on the natural index ordering within the set of semipolarized bit-channels. For reference, we present the results for conventional $(1024, 512)$ polar codes obtained using SCL [4], BPL [13] and CA-SCL decoding with 16 CRC bits [4]. Solid lines correspond to augmented codes, while dashed lines are for conventional polar codes.

At FER = 10^{-3}, the OPSS design and NDE design offer gains of 0.12 dB and 0.18 dB over the conventional DE design, respectively. At this FER they also perform comparably to SCL decoding, although SCL becomes superior at higher FERs. We remark that when the outer codes designed using the OPSS and NDE methods are disconnected from the concatenation architecture, their performance is inferior to that of a code designed using conventional DE. This confirms their inherent relationship with the concatenation structure.

Figs. 15(a) and 15(b) present the results for local and global decoding, respectively, for a local-global code with component code lengths $N_0 = 256, N_1 = N_2 = 1024$. The connections between the inner codes and the outer code are

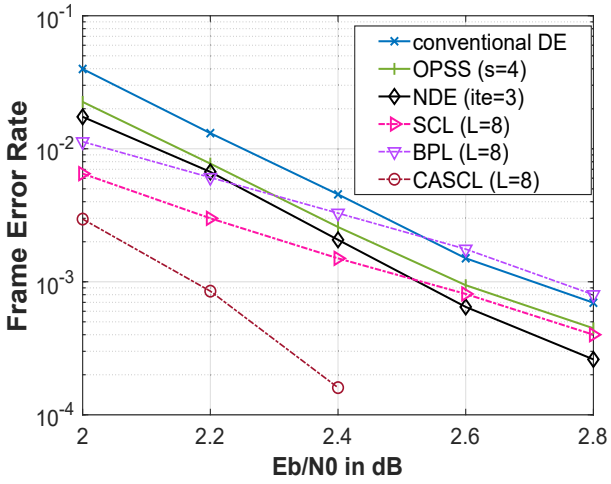

Fig. 14: Augmented code N_0=64, N_1=1024 with natural interleaver.

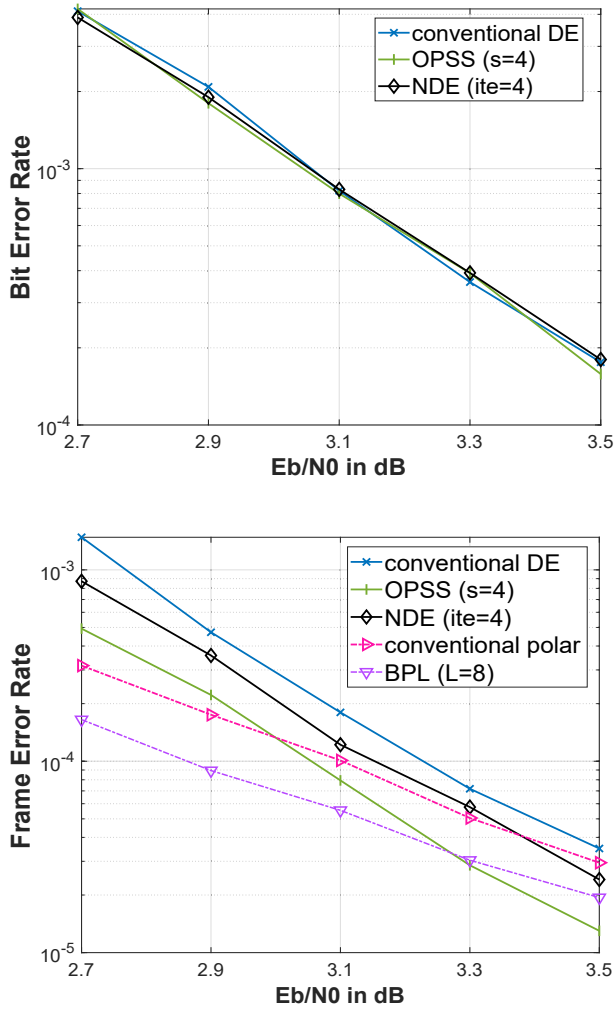

(b) global decoding results

Fig. 15: Local-global code with $N_0 = 256, N_1 = N_2 = 1024$.

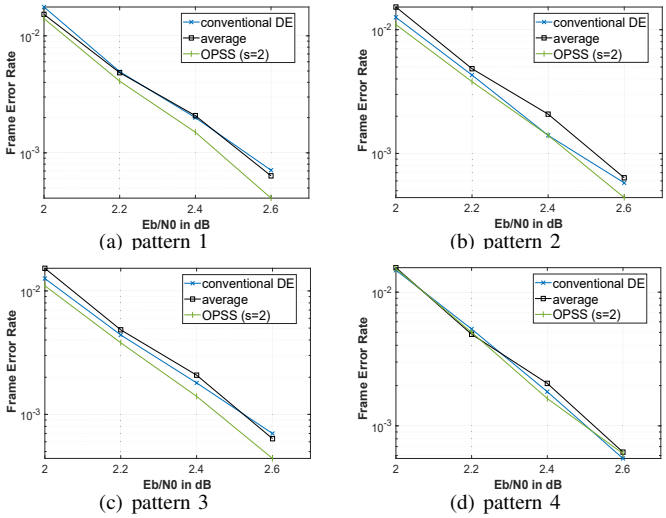

(a) pattern 1 (b) pattern 2 (c) pattern 3 (d) pattern 4

Fig. 16: Augmented code $N_0 = 64, N_1 = 1024$ with different interleaver patterns.

as described by Example III.2 in [21]. Local decoding results for the different outer code design methods are similar, as expected, since local decoding does not rely on the outer code. Under global decoding, at FER = 10^{-4}, the OPSS and NDE designs provide gains of 0.19 dB and 0.07 dB over conventional DE, respectively. The results for conventional $(2048, 1024)$ polar codes obtained using BP and BPL [13] decoding are shown for reference. Solid lines represent local-global codes, while dashed lines indicate conventional polar codes. In summary, the improved global decoding performance provided by the new outer code constructions does not reduce the local decoding performance.

Although the natural ordering is attractive from an implementation standpoint, it may not provide the best starting point for these design methods, and experiments with other connection patterns, both structured and randomly generated, show that gains achieved with the proposed methods vary. For example in Fig. 16, we selected four different patterns for augmented codes whose performance are close to the average of all the interleaver patterns, within which pattern 1 and 3 benefit from OPSS. These results suggest that while some interleavers benefit from the proposed method, others might not experience the same level of enhancement. This highlights the importance of selecting an appropriate outer code design method that aligns well with the connection pattern. How to jointly optimize the interleaver pattern and the design methods remains a problem for further research.

VII. Conclusion

In this paper, we proposed four bounds on the value of $|MVSS(\mathcal{J})|$, which can be used to bound the stopping distance of concatenated polar codes. We proposed a design method for the outer code in augmented and local-global polar code architectures based on the "stopping distance" associated with each bit position. However, several questions still remain to be answered:

- In Section III, a practical algorithm for computing $|MVSS'(\mathcal{J}_{out})|$ remains to be found.

- In Section IV, a practical algorithm for computing $|MVSS(\mathcal{J})|$ remains to be found. A potential direction for future research could involve proving the NP-hardness of this problem.
- In Fig. 8, we only proved the tightness for Lower Bound I. However, it appears that Deletion Bound I is also tight under certain conditions, as indicated by the following conjecture.

Conjecture 1. *If set $\mathcal{J}$ satisfies both cover condition and swap condition, then Algorithm 1 (Deletion Bound I) can find the exact value of $|MVSS(\mathcal{J})|$.*

APPENDIX

Proof of Theorem 8: The proof proceeds by induction. For the case $n = 1$, the statement follows immediately from inspection of the corresponding factor graph. Now, suppose the result is true for a given n. By the induction hypothesis, $|MVSS(\mathcal{J}_n)| = \min_{i\in\mathcal{J}_n} f(i)$ holds if $\mathcal{J}_n$ satisfies both conditions. Now, for a set $\mathcal{J}_{n+1}$ that also satisfies both conditions, consider the following cases:

1. $|\overline{\mathcal{J}_{n+1}}| = 0$. There is no information bit on the upper-half of the leftmost stage within the factor graph. Clearly $\mathcal{J}^U_{n+1}$ and $\mathcal{J}^L_{n+1}$ are identical, and $\mathcal{J}^U_{n+1} = \mathcal{J}^L_{n+1} = \underline{\mathcal{J}_{n+1}}$. We state that both of them would be in the stopping set corresponding to $MVSS(\mathcal{J}_{n+1})$, which is because all the neighbor check nodes in $UT(\mathcal{J}_{n+1})$ that are on the left of $\mathcal{J}^U_{n+1}$ and $\mathcal{J}^L_{n+1}$ are degree two. An example can be seen in Fig. 17(a), where $UT(\mathcal{J}_{n+1})$ is labeled by black nodes.

From Proposition 3, we know that $\mathcal{J}^U_{n+1}$ and $\mathcal{J}^L_{n+1}$ satisfy both conditions, thus

$$|MVSS(\mathcal{J}^L_{n+1})| = |MVSS(\mathcal{J}^U_{n+1})| = \min_{i\in\underline{\mathcal{J}_{n+1}}} f(i).$$

Now we prove that $\min_{i\in\underline{\mathcal{J}_{n+1}}} f(i) = \frac{1}{2}\min_{i\in\mathcal{J}_{n+1}} f(i)$. Assume $MIB^*(\mathcal{J}_{n+1}) = j^*$, then we state that $MIB^*(\underline{\mathcal{J}_{n+1}}) = \underline{j^*}$. Because if there exists $k \in \mathcal{J}_{n+1}$ such that $f(\underline{k}) < f(\underline{j^*})$, then $f(k) = 2 \times f(\underline{k}) < 2 \times f(\underline{j^*}) = f(j^*)$, which contradicts the assumption that j^* is the MIB. Now, since $f(j^*) = 2\times f(\underline{j^*})$, we know that $|MVSS(\mathcal{J}_{n+1})| = 2 \times |MVSS(\underline{\mathcal{J}_{n+1}})| = 2 \times f(\underline{j^*}) = f(j^*)$.

2. $|\overline{\mathcal{J}_{n+1}}| \geq |\underline{\mathcal{J}_{n+1}}|$. There are more information bits on the upper-half than on the lower-half. We prove that this case is impossible unless $\mathcal{J}_{n+1}$ contains all the positions on the left (code rate is 1). According to the cover condition, any $i \in \overline{\mathcal{J}_{n+1}}$ would imply that $i+2^n \in \underline{\mathcal{J}_{n+1}}$, thus $|\overline{\mathcal{J}_{n+1}}| \leq |\underline{\mathcal{J}_{n+1}}|$.

Now we assume that $|\overline{\mathcal{J}_{n+1}}| = |\underline{\mathcal{J}_{n+1}}|$, which implies that $j \in \mathcal{J}_{n+1} \Rightarrow \underline{j} \in \mathcal{J}_{n+1}$. We also assume that j^* has the minimum weight (fewest number of 1's in the binary expression $(j^*)_b$) among all $j \in \underline{\mathcal{J}_{n+1}}$. Clearly $wt((j^*)_b) \geq 1$ since $j^* \geq 2^n$. We further assume that $wt((j^*)_b) > 1$. By the definition of $\underline{j^*}$, it directly follows that $wt((\underline{j^*})_b) = wt((j^*)_b) - 1 \geq 1$. We also know that the last bit of the binary representation of $\underline{j^*}$ is 0, i.e., $(\underline{j^*})_n = 0$. Without loss of generality, assume $(\underline{j^*})_m = 1, m < n$. Then, we can swap $(\underline{j^*})_m$ with $(\underline{j^*})_n$ to get a new index l. According to the swap condition, $l \in \mathcal{J}_{n+1}$ and since $l_n = 1$, we have $l \in \underline{\mathcal{J}_{n+1}}$.

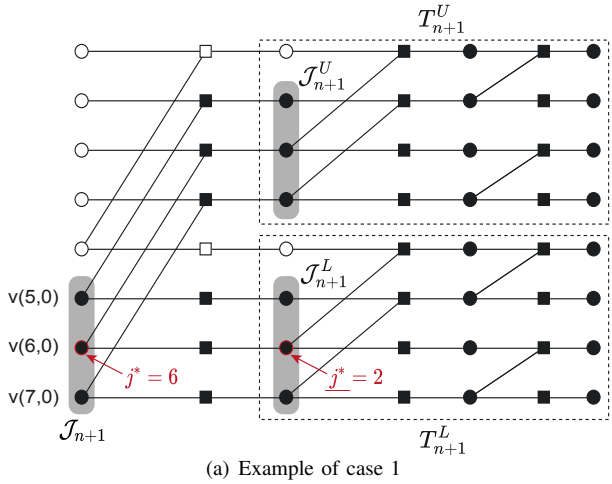

(a) Example of case 1

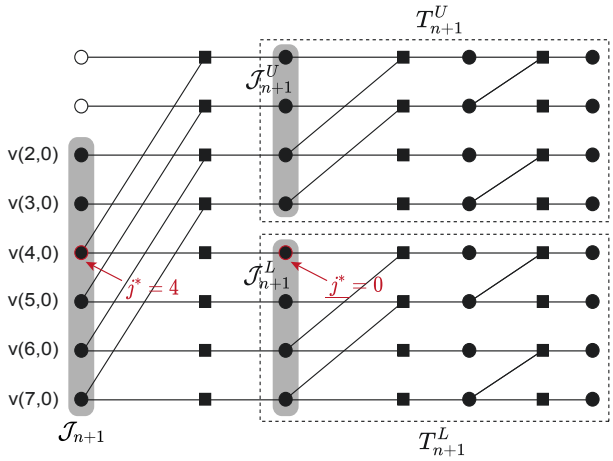

(b) Example of case 3

Fig. 17: Illustrative examples for the proof of Theorem 8.

Now $wt(l_b)$ is smaller than $wt((j^*)_b)$, which contradicts the assumption.

If $wt((j^*)_b) = 1$, then $j^* = 2^n$ and by the cover condition we know that $0 \in \mathcal{J}_{n+1}$, which implies that $\mathcal{J}_{n+1}$ contains all bits on the left. It is trivial to see that $|MVSS(\mathcal{J}_{n+1})| = \min_{i\in\mathcal{J}_{n+1}} f(i) = f(0) = 1$.

3. $0 < |\overline{\mathcal{J}_{n+1}}| < |\underline{\mathcal{J}_{n+1}}|$. Let $MIB^*(\mathcal{J}_{n+1}) = j^*$. An example for this case is shown in Fig. 17(b). We first state that $j^* \geq 2^n$. Otherwise if $j^* < 2^n$, we can swap a 1 to the last bit to get another index l, such that $l > j^*$. From (1), we know that $f(l) = f(j^*)$ since $wt(l_b) = wt((j^*)_b)$. This contradicts the definition of MIB^* as the MIB with the largest index.

Again we have $\mathcal{J}^U_{n+1} = \mathcal{J}^L_{n+1} = \underline{\mathcal{J}_{n+1}}$, since any $j \in \overline{\mathcal{J}_{n+1}}$ would imply that $j + 2^n \in \mathcal{J}_{n+1}$, according to the cover condition. Similar to case 1, we can conclude that $MIB^*(\underline{\mathcal{J}_{n+1}}) = \underline{j^*}$, using the same proof.

Now the difference with case 1 is: $\mathcal{J}^U_{n+1}$ might not be in the stopping set corresponding to $MVSS(\mathcal{J}_{n+1})$, since there are some degree-3 neighbor check nodes on the left of $\mathcal{J}^U_{n+1}$ so that some nodes in $\mathcal{J}^U_{n+1}$ may be excluded from the stopping set corresponding to $MVSS(\mathcal{J}_{n+1})$. Denote by $\mathcal{S}$ an arbitrary subset of $\mathcal{J}^U_{n+1}$. From Theorem 1, we know that $|MVSS(\mathcal{S})| \geq \min_{s\in\mathcal{S}} f(s)$. Since $\mathcal{S} \subseteq \mathcal{J}^U_{n+1}$, we have

$|MVSS(\mathcal{S})| \geq \min_{s\in\mathcal{S}} f(s) \geq \min_{i\in\mathcal{J}_{n+1}^U} f(i) = f(\underline{j^*})$, which suggests that the minimum size we can expect in T_{n+1}^U is actually $f(\underline{j^*})$. Then, the lower-half factor graph T_{n+1}^L can be treated as incase 1, and we have $|MVSS(\mathcal{J}_{n+1})| = 2 \times |MVSS(\underline{\mathcal{J}_{n+1}})| = 2 \times f(\underline{j^*}) = f(j^*)$.

■

Acknowledgment

This work was supported in part by the National Science Foundation under grants CCF-1764104, CCF-2212437, and CCF-2416362. Furthermore, we would like to thank the anonymous reviewers for their valuable comments that helped to improve this paper.

References

[1] E. Arıkan, "Channel polarization: A method for constructing capacity-achieving codes for symmetric binary-input memoryless channels," *IEEE Trans. Inf. Theory*, vol. 55, no. 7, pp. 3051-3073, Jul. 2009.

[2] E. Arıkan, "Systematic polar coding," *IEEE Commun. Lett.*, vol. 15, no. 8, pp. 860-862, Aug. 2011.

[3] T. Wang, D. Qu, and T. Jiang, "Parity-check-concatenated polar codes," *IEEE Commun. Lett.*, vol. 20, no. 12, pp. 2342-2345, Dec. 2016.

[4] I. Tal and A. Vardy, "List decoding of polar codes," *IEEE Trans. Inf. Theory*, vol. 61, no. 5, pp. 2213-2226, May. 2015.

[5] A. Eslami and H. Pishro-Nik, "On finite-length performance of polar codes: Stopping sets, error floor, and concatenated design," *IEEE Trans. Commun.*, vol. 61, no. 3, pp. 919-929, Mar. 2013.

[6] M. Bakshi, S. Jaggi, and M. Effros, "Concatenated polar codes," in *Proc. IEEE Int. Symp. Inf. Theory (ISIT)*, Jun. 2010, pp. 918-922.

[7] J. Guo, M. Qin, A. Guillén i Fàbregas, and P. H. Siegel, "Enhanced belief propagation decoding of polar codes through concatenation," in *Proc. IEEE Int. Symp. Inf. Theory (ISIT)*, Jun.-Jul. 2014, pp. 2987-2991.

[8] A. Elkelesh, M. Ebada, S. Cammerer, and S. t. Brink, "Flexible length polar codes through graph based augmentation," in *Proc. 11th Int. ITG Conf. on Syst., Commun. and Coding (SCC 2017)*, Feb. 2017, pp. 1-6.

[9] Z. Zhu, W. Wu, and P. H. Siegel, "Polar codes with local-global decoding," in *Proc. 56th Asilomar Conf. Signals Syst. Comput.*, Oct. 2022, pp. 392-396.

[10] E. Arıkan, "Polar codes: A pipelined implementation," in *Proc. Int. Symp. Broadcast Commun. (ISBC)*, Jul. 2010, pp. 11–14.

[11] Z. Li, Y. Shen, Y. Ren, Y. Huang, X. You, and C. Zhang, "Belief propagation decoding for short-length codes based on sparse Tanner graph," *IEEE Commun. Lett.*, vol. 28, no. 5, pp. 969-973, May. 2024.

[12] A. Elkelesh, M. Ebada, S. Cammerer, and S. t. Brink, "Belief propagation list decoding of polar codes," *IEEE Commun. Lett.*, vol. 22, no. 8, pp. 1536-1539, Aug. 2018.

[13] B. Li, B. Bai, M. Zhu, and S. Zhou, "Improved belief propagation list decoding for polar codes," in *Proc. IEEE Int. Symp. Inf. Theory (ISIT)*, Los Angeles, USA, Jun. 2020, pp. 413-418.

[14] R. Mori and T. Tanaka, "Performance of polar codes with the construction using density evolution," *IEEE Commun. Lett.*, vol. 13, no. 7, pp. 519-521, Jul. 2009.

[15] S.-Y. Chung, T. J. Richardson, and R. L. Urbanke, "Analysis of sum-product decoding of low-density parity-check codes using a Gaussian approximation," *IEEE Trans. Inf. Theory*, vol. 47, no. 2, pp. 657-670, Feb. 2001.

[16] J. Dai, K. Niu, Z. Si, C. Dong, and J. Lin, "Does Gaussian Approximation work well for the long-length polar code construction?," *IEEE Access*, vol. 5, pp. 7950-7963, Apr. 2017.

[17] C. Schürch, "A partial order for the synthesized channels of a polar code," in *Proc. IEEE Int. Symp. Inf. Theory (ISIT)*, Jul. 2016, pp. 220-224.

[18] M. Bardet, V. Dragoi, A. Otmani, and J.-P. Tillich, "Algebraic properties of polar codes from a new polynomial formalism," in *Proc. IEEE Int. Symp. Inf. Theory (ISIT)*, Jul. 2016, pp. 230-234.

[19] W. Wu and P. H. Siegel, "Generalized partial orders for polar code bit-channels," *IEEE Trans. Inf. Theory*, vol. 65, no. 11, pp. 7114-7130, Nov. 2019.

[20] W. Wu, Z. Zhai, and P. H. Siegel, "Improved hybrid RM-polar codes and decoding on stable permuted factor graphs," in *Proc. IEEE 10th Int. Symp. on Topics in Coding (ISTC)*, Aug. 2021, pp. 1-5.

[21] Z. Zhu and P. H. Siegel, "Outer code designs for augmented and local-global polar code architectures," *Proc. IEEE Int. Symp. Inf. Theory (ISIT)*, pp. 2418-2423, Jul. 2024.

[22] Z. Zhu and P. H. Siegel, "Outer code designs for augmented and local-global polar code architectures," arXiv:2402.04486 [cs.IT], May 2024.

Ziyuan Zhu (Student Fellow, IEEE) received his B.E. in electrical communication engineering from Xi'an Jiaotong University, Xi'an, China, in 2021, and the M.S. in electrical and computer engineering from the University of California San Diego, San Diego, CA, USA, in 2023, where he is currently pursuing the Ph.D. degree with the department of electrical and computer engineering. He is also with the center for memory and recording research (CMRR), University of California San Diego. His research focuses on the application of error correction codes in storage systems, particularly polar and polar-like codes, with an emphasis on developing low-complexity decoding algorithms and efficient code constructions.

Paul H. Siegel (Life Fellow, IEEE) received the S.B. and Ph.D. degrees in Mathematics from the Massachusetts Institute of Technology, Cambridge, MA, USA, in 1975 and 1979, respectively. He held a Chaim Weizmann Postdoctoral Fellowship with the Courant Institute, New York University, New York, NY, USA. He was with the IBM Research Division, San Jose, CA, USA, from 1980 to 1995. He joined the faculty at the University of California San Diego (UCSD), La Jolla, CA, USA, in 1995, where he is currently a Distinguished Professor of Electrical and Computer Engineering with the Jacobs School of Engineering. He is affiliated with the Center for Memory and Recording Research where he holds an Endowed Chair and served as Director from 2000 to 2011. His research interests include information theory, coding techniques, and machine learning, with applications to digital data storage and transmission. He is a Member of the National Academy of Engineering. He was a Member of the Board of Governors of the IEEE Information Theory Society from 1991 to 1996 and from 2009 to 2014. He was the 2015 Padovani Lecturer of the IEEE Information Theory Society. He was a co-recipient of the 1992 IEEE Information Theory Society Paper Award, the 1993 IEEE Communications Society Leonard G. Abraham Prize Paper Award, and the 2007 Best Paper Award in Signal Processing and Coding for Data Storage from the Data Storage Technical Committee of the IEEE Communications Society. He served as an Associate Editor of Coding Techniques of the IEEE TRANSACTIONS ON INFORMATION THEORY from 1992 to 1995, and as the Editor-in-Chief from 2001 to 2004. He has served as Co-Guest Editor of special issues for the IEEE TRANSACTIONS ON INFORMATION THEORY, the IEEE JOURNAL ON SELECTED AREAS IN COMMUNICATIONS (twice), the IEEE JOURNAL ON SELECTED AREAS IN INFORMATION THEORY, the IEEE TRANSACTIONS ON MOLECULAR, BIOLOGICAL, AND MULTI-SCALE COMMUNICATIONS, and IEEE BITS THE INFORMATION THEORY MAGAZINE.